

## Supplementary information for “Quantifying the origin of inter-adsorbate interactions on reactive surfaces for catalyst screening and design”

### I. Charge on the adsorbed species

To calculate the formal charge on the adsorbed H<sub>2</sub>S molecules, we performed a Bader charge analysis on each H<sub>2</sub>S molecule at different coverage values and compared the net charge inside the Bader surface to that of an isolated H<sub>2</sub>S molecule in vacuum.

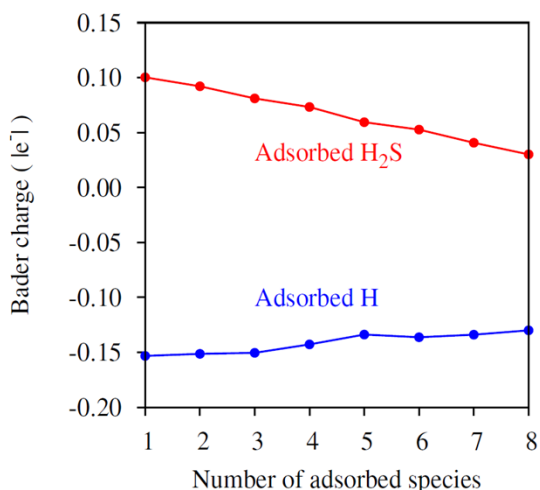


Figure S1: The average Bader charge on any adsorbed H<sub>2</sub>S molecule is less than 0.1 e<sup>-</sup> more than that on an isolated H<sub>2</sub>S molecule (dashed red line). This low formal charge indicates that Coulombic repulsion cannot be a significant contributor to the inter-adsorbate interaction observed here. This is supported by the fact that the nominal Bader charge on each adsorbed H atom is approximately 0.15 e<sup>-</sup> greater than that of an isolated H atom, but adsorbed H atoms do not demonstrate any noticeable inter-adsorbate interaction.

### II. Effect of adsorbate-induced change in surface electronic structure

To calculate the impact of adsorbate-induced change in the surface electronic structure on the effective inter-adsorbate interaction, a two-part calculation was performed. In the first part, the dependence of adsorption energy on an electronic structure metric is determined. Following the d-band theory, the metric chosen is the distance between the center of the Fe 3d band and the Fermi level. From Figure S2(a), we obtain the relation  $E_{ads} = 1.97E_{DBC} - 1.86 \text{ eV}$ , where  $E_{ads}$

is the adsorption energy per H<sub>2</sub>S molecule and  $E_{DBC}$  is the distance between the center of the Fe 3d band and the Fermi level.

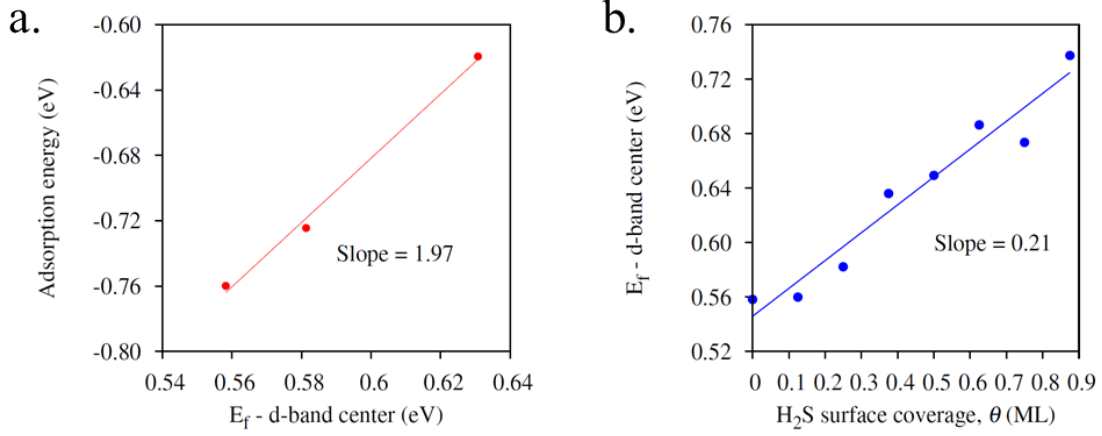


Figure S2: (a) The adsorption energy of H<sub>2</sub>S depends linearly upon the distance between the d-band center and the fermi level. (b) The chosen electronic structure metric varies linearly with the surface coverage of H<sub>2</sub>S. A combination of these two factors is largely responsible for the observed variation in adsorption energy with increasing H<sub>2</sub>S surface coverage.

In the second part of calculation, the relation between the H<sub>2</sub>S surface coverage and the electronic structure metric ( $E_{DBC}$ ) is identified. From Figure S2(b), we get  $E_{DBC} = 0.21\theta + 0.55$  eV, where  $\theta$  is the surface coverage in monolayers.

From a product of these two linear relations, we get  $E_{ads} \propto 0.41\theta$ , which represents about 75% of the observed overall dependence of adsorption energy on surface coverage shown in Figure 6 in the manuscript.

### III. Random sampling of adsorbate configuration phase-space

One simple alternative to using cluster expansion methods is to randomly sample the adsorbate configuration at different coverage values, e.g. for a coverage of 0.5, a configuration consisting of adsorbates randomly distributed over half of the available adsorption sites is used to calculate adsorption energy according to Equation 1 in the article. While this approach has the advantage of bypassing the somewhat time consuming cluster expansion sampling, this method is unlikely

to calculate the ground state energy at any coverage value. In Figure S3 (a), we can see that a random sampling adsorbate configurations leads to an underestimation of the curvature in the energy-coverage curve, which is a measure of the inter-adsorbate interaction. This failure to sample the ground state introduces corresponding errors in the calculation of adsorption energy. These are highlighted in Figure S3 (b), where temperature programmed desorption spectra calculated using adsorption energies from randomly-sampled structures is compared to experimental data. It can be easily seen that the correspondence of peak position with the experimental spectrum is much better for adsorption energies predicted by cluster expansion.

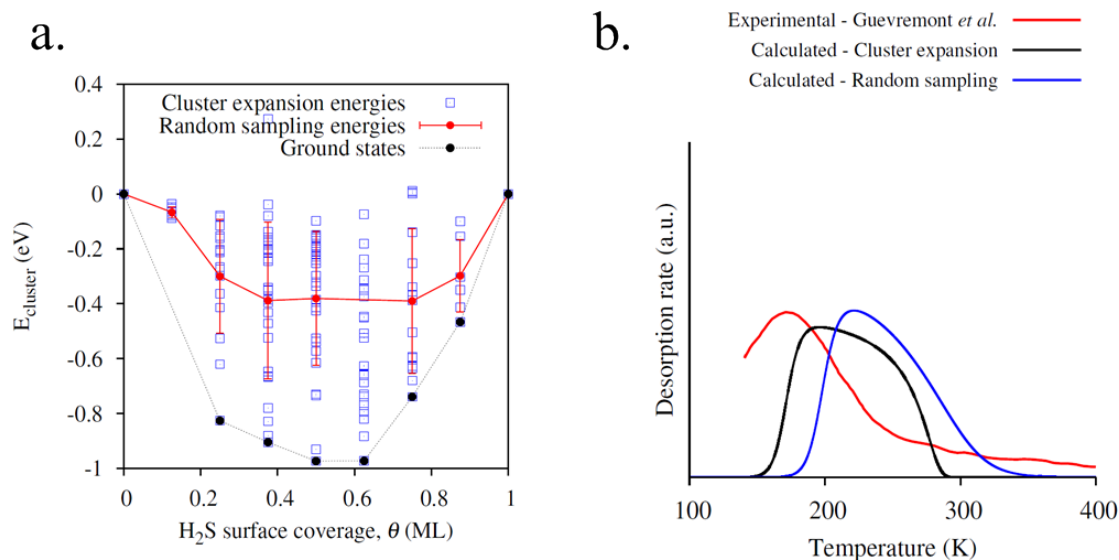


Figure S3: (a) Random sampling of adsorbate structures underestimates inter-adsorbate interactions as it does not directly sample the ground state configuration and energy. Large errors are associated with random sampling of the phase space, as indicated by the size of the error bars. (b) TPD spectrum based on adsorption energies calculated from a random sampling of the adsorbate configuration phase space does not agree with the experimental spectrum in terms of the peak position.

#### IV. Convergence of DFT calculations with respect to simulation parameters

As mentioned in the text, coverage-dependent adsorption energy of H<sub>2</sub>S molecules is performed using wavefunctions expanded in plane waves with components up to 350 eV and using a 3x3x1 Monkhorst Pack grid to sample the reciprocal space. To test the sensitivity of the calculated adsorption energies to these simulation parameters, we compare the adsorption energy reported in the main text to calculations using a higher plane-wave cutoff energy (Figure S4) and to calculations which include a denser Monkhorst Pack k-point grid (5x5x1) to sample the reciprocal space (Figure S5). Both figures show that the calculations reported in the main text are converged with respect to the plane-wave cutoff as well as the reciprocal space sampling.

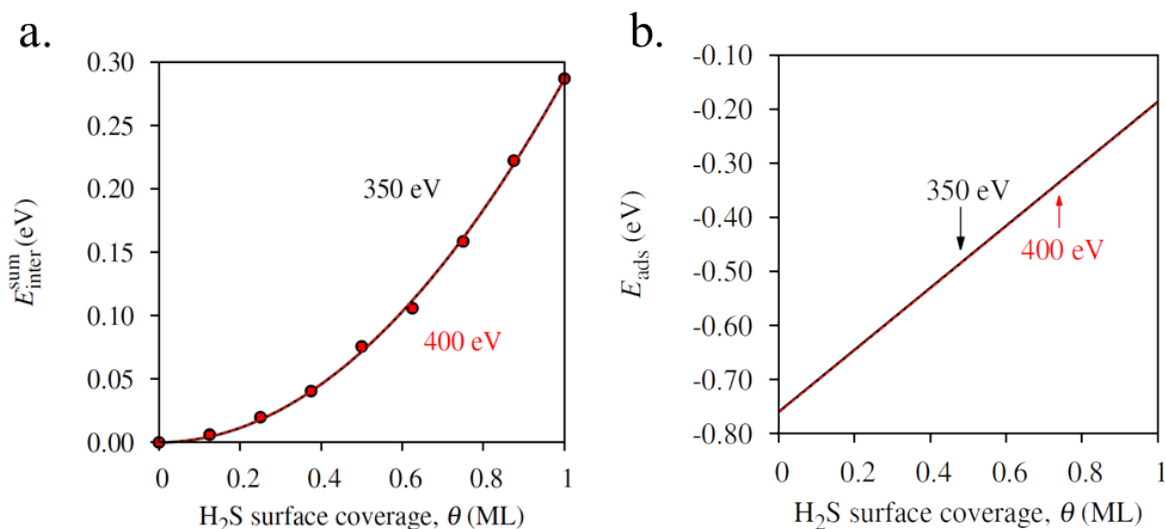


Figure S4: A comparison of cumulative inter-adsorbate interactions (a) and adsorption energy (b) from DFT calculations performed using a 350 eV (black, solid line) and 400 eV (red, dashed line) plane wave cutoffs shows that 350 eV calculations (used in the main text) are well converged with respect to the energy cutoff.

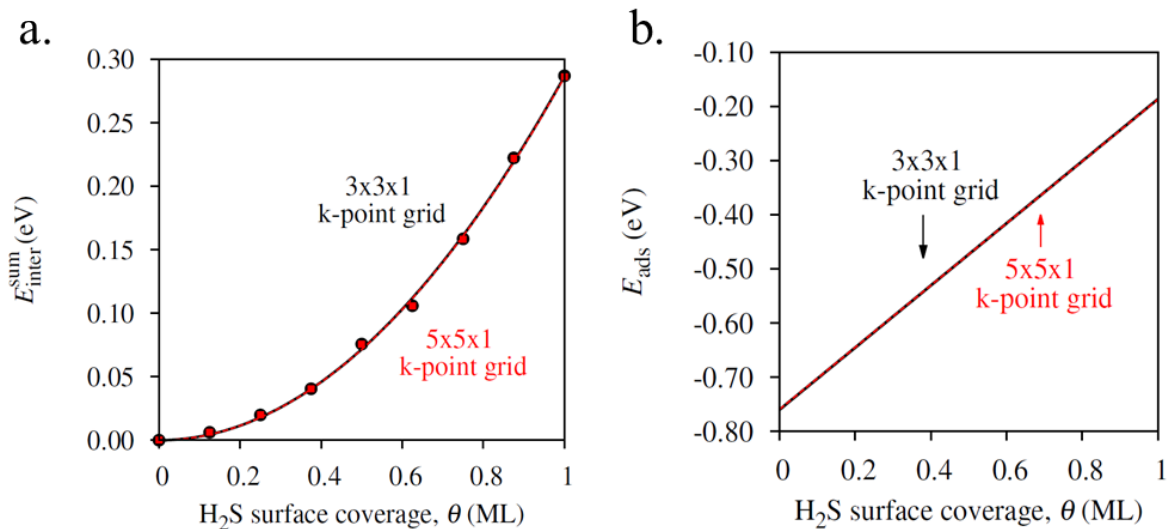


Figure S5: A comparison of cumulative inter-adsorbate interactions (a) and adsorption energy (b) from DFT calculations performed using a 3x3x1 (black, solid line) and 5x5x1 (red, dashed line) reciprocal space sampling grids shows that calculations based on the 3x3x1 Monkhorst Pack grids (used in the main text) are well converged with respect to reciprocal-space sampling.

## V. Quantification of attractive inter-adsorbate interactions

The approach used to quantify steric interactions between H<sub>2</sub>S adsorbates in Section II. b. of the main text (i.e. the calculation of interaction energies in the absence of the FeS<sub>2</sub> surface) strictly captures all through-space interactions between adsorbate molecules. This includes repulsive steric interactions as well as attractive hydrogen bonding and (to the incomplete extent that the PBE functional includes it) dispersion interactions.

Figure S6 shows the cumulative through-space interadsorbate interactions for an ensemble of H<sub>2</sub>O molecules (i.e. the analysis in Section II b. of the main text is repeated for H<sub>2</sub>O molecules instead of H<sub>2</sub>S molecules). In contrast to H<sub>2</sub>S molecules, the compact charge distributions and more polar bonds of water molecules ensure that H-bonds (and not steric interactions) are the dominant through-space interactions. As a result the expression for  $E_{\text{inter}}^{\text{sum}}$  shows a net attractive interaction in the case of H<sub>2</sub>O molecules.

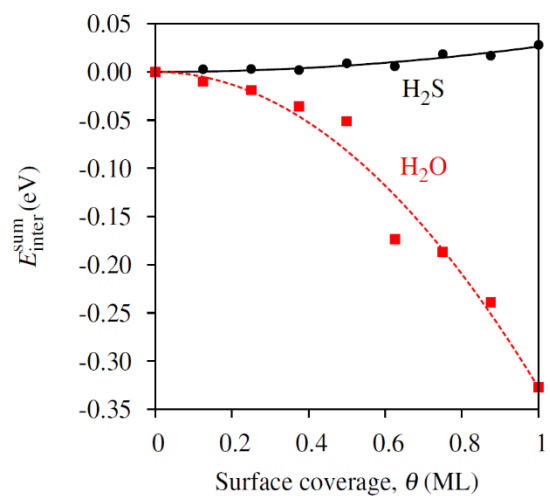


Figure S6: Cumulative inter-adsorbate interactions for  $\text{H}_2\text{S}$  and  $\text{H}_2\text{O}$  molecules in the absence of the  $\text{FeS}_2$  surface. The compact  $\text{H}_2\text{O}$  molecules experience attractive H-bond interactions and negligible steric interactions, while the larger, less polar  $\text{H}_2\text{S}$  molecules experience stronger steric interactions